# Review of constituent retrieval in optically deep and complex waters from satellite imagery

Odermatt, D ; Gitelson, Anatoly ; Brando, Vittorio Ernesto ; Schaepman, Michael E

DOI: https://doi.org/10.1016/j.rse.2011.11.013

# Review of constituent retrieval in optically deep and complex waters from satellite imagery

Daniel Odermatt[1,*], Anatoly Gitelson[2], Vittorio Ernesto Brando[3], Michael Schaepman[1]

[1]Remote Sensing Laboratories, University of Zurich, Switzerland

[2]School of Natural Resources, University of Nebraska, Lincoln, Nebraska, United States

[3]CSIRO Land and Water, Environmental Earth Observation Programme, Canberra, Australian Capital Territory 2601, Australia

* Corresponding author. Tel.: +41 446356517; fax: +41 446356846.

E-mail address: daniel.odermatt@geo.uzh.ch

## Abstract

We provide a comprehensive overview of water constituent retrieval algorithms and underlying definitions and models for optically deep and complex (i.e. case 2) waters using earth observation data. The performance of constituent retrieval algorithms is assessed based on matchup validation experiments published between January 2006 and May 2011. Validation practices range from singular vicarious calibration experiments to comparisons using extensive in situ time series. Band arithmetic and spectral inversion algorithms for all water types are classified using a method based scheme that supports the interpretation of algorithm validity ranges. Based on these ranges we discuss groups of similar algorithms in view of their strengths and weaknesses. Such quantitative literature analysis reveals clear application boundaries. With regard to chlorophyll retrieval, validation of blue-green band ratios in coastal waters is limited to

oligotrophic, predominantly ocean waters, while red-NIR ratios apply only at more than 10 mg/m$^3$. Spectral inversion techniques – although not validated to the same extent – are necessary to cover all other conditions. Suspended matter retrieval is the least critical, as long as the wavelengths used in empirical models are increased with concentrations. The retrieval of dissolved organic matter however remains relatively inaccurate and inconsistent, with large differences in the accuracy of comparable methods in similar validation experiments. We conclude that substantial progress has been made in understanding and improving retrieval of constituents in optically deep and complex waters, enabling specific solutions to almost any type of optically complex water. Further validation and intercomparison of spectral inversion procedures is however needed to learn if solutions with a larger validity range are feasible.

# 1 Introduction

Optically deep and complex waters are referred to as case 2 waters, as opposed to phytoplankton dominated case 1 waters of the open ocean (Morel and Prieur, 1977). The variety within case 2 waters is large, because concentrations as well as specific inherent optical properties of chlorophyll (*CHL*), total suspended matter (*TSM*) and coloured dissolved organic matter concentrations (*CDOM*) are subject to potentially large and independent variations. Satellite sensors such as SeaWiFS, MODIS, and MERIS are currently being used to deliver ocean color data, attaining the requirements necessary for ocean biogeochemistry and climate research (Dierssen, 2010; McClain, 2009). Alas, universally applicable algorithms for the retrieval of water constituents from case 2 waters are not known (IOCCG, 2006, 2009). Specific algorithms are thus optimized and validated for commonly understood but ill-defined water types, e.g. turbid (Gitelson et al., 2007) or clear water (Belzile et al., 2004). Other authors address

trophic classes (Cheng Feng et al., 2009; Dekker and Peters, 1993; Iluz et al., 2003), for which several diverging definitions exist (Bukata et al., 1995; Carlson and Simpson, 1996; Chapra and Dobson, 1981; Nürnberg, 1996; Wetzel, 1983). Trophic thresholds vary however with ecosystem specific limitations to primary productivity, while the validity of remote sensing algorithms is determined only by the variability in optical properties.

Carder et al. (1999) and Morel (1980) distinguish empirical and analytical methods for water constituent retrieval, and in-betweens with the epithet "semi-". Empirical algorithms are derived by statistical regression (Kabbara et al., 2008; Mahasandana et al., 2009) or endmember selection (Tyler et al., 2006), which implies effective data optimization but limited transferability (Austin and Petzold, 1981). Analytical algorithms are based on simplified solutions of the radiative transfer equation. This usually requires approximations or calibration with empirical coefficients (Carder et al., 1999), while statistical regression often leads to solutions that coincide with properties known from physical models (e.g. normalizing band ratios (Gitelson, 1992)), explaining the epithet "semi-" from either side. Either type of algorithm is usually applied as a band arithmetic solution for one constituent at a time, although empirical solutions can also be found by other approaches (Gonzalez Vilas et al., 2011; Tyler et al., 2006).

In contrast, spectral inversion procedures match spectral measurements with bio-optical forward models by means of inversion techniques. The spectral inherent optical properties (IOPs, (Preisendorfer, 1961)) of all three constituents are thereby retrieved at once from one spectral apparent property (AOP). Several inversion techniques are applied for this procedure, whereby the investigated AOP is matched with simulated AOPs from bio-optical forward models, i.e. either analytical relationships (Albert and Mobley, 2003; Gordon et al., 1975; Lee et al., 2002; Maritorena et al., 2002; Park and

Ruddick, 2005) or numerical radiative transfer models (Bulgarelli et al., 1999; Jin and Stamnes, 1994; Mobley, 1989; Zhai et al., 2010).

By comprehensively reviewing the literature from 2006 to May 2011, we discuss in this paper recent studies reporting matchup validation results for water constituent retrieval in case 2 waters from satellite imagery using band ratio or spectral inversion algorithms. Accuracy assessments for band ratio or spectral inversion algorithms based only on in situ measurements, e.g. Kostadinov et al. (2007)), Moore et al. (2009) or Shanmugam (2010) or simulated datasets, e.g. Qin et al. (2007) are not discussed. We apply a quantitative review approach on validation experiments published from 2006 to May 2011, although the algorithms used thereby may date further back. A temporally more comprehensive, qualitative review in line with earlier work by Dekker et al. (1995) has very recently been published by Matthews (2011).

We group the paper in 7 sections, where the relevance of IOPs and AOPs in models and algorithms are discussed first, followed by a description of band arithmetic and spectral inversion algorithms. Recent validation experiments for either approach are then summarized and quantitatively analyzed for their range of applicability.

## 2 Relevance of IOPs in models and algorithms

Regarding IOPs, the volume scattering function $\beta(\psi)$ is the elementary property for the integration of the scattering and backscattering coefficients $b$ and $b_b$, respectively, over scattering angle $\psi$. Measurements of $\beta(\psi)$ (Chami et al., 2006; Freda et al., 2007; Freda and Piskozub, 2007; Lee and Lewis, 2003; Petzold, 1972; Sokolov et al., 2010; Sullivan and Twardowski, 2009) are normalized to the scattering phase function $\tilde{\beta}(\psi)$. Several models of $\tilde{\beta}(\psi)$ have been proposed to approximate these measurements (Fournier and Forand, 1994; Fournier and Jonasz, 1999; Haltrin, 2002; Mobley et al., 1993). Their

effect on calculated reflectance quantities is up to 20% (Chami et al., 2006; Gordon, 1993; Mobley et al., 2002; Morel et al., 2002; Morel and Gentili, 1996). The ratio of molecular to total scattering, $\eta$, is a major proxy for the shape of $\beta(\psi)$, since molecular $\tilde{\beta}_W$ is less anisotropic than particulate $\tilde{\beta}_{TSM}$ (Morel, 1974; Smith and Baker, 1981). The absorption coefficient $a$ in contrast is omnidirectional, but influences the intensity and anisotropy of reflectance through the single scattering albedo $\omega_0$ (Gordon and Brown, 1973; Gordon et al., 1975; Morel and Prieur, 1977) and the number of subsequent scattering events of a photon before reaching the interface, $N$ (Loisel and Morel, 2001; Morel et al., 2002), respectively. An alternative term for the former is the single backscattering albedo $\omega_b$. The latter indicates the blurring of $\beta(\psi)$ in turbid water (Pfeiffer and Chapman, 2008; Piskozub and McKee, 2011; Sydor, 2007).

The ability to account for variations in these IOPs is limited for band arithmetic algorithms, while increasingly addressed by spectral inversion algorithms for radiative transfer simulations (Doerffer and Schiller, 2007; Schroeder et al., 2007b; Van Der Woerd and Pasterkamp, 2008) or specific semi-analytical models (Albert and Mobley, 2003; Park and Ruddick, 2005).

# 3 Relevance of AOPs in models and algorithms

The first widely used AOP is the bihemispherical irradiance reflectance $R^-$, which is related to $\omega_b$ in the earliest semi-analytical models for case 2 water by means of the linear coefficient $f$ (Gordon et al., 1975; Morel and Prieur, 1977), which again varies with illumination zenith angle $\theta_s^+$ (Gordon, 1989; Kirk, 1991; Sathyendranath and Platt, 1997).

Subsequent experiments for case 1 (Morel and Gentili, 1991, 1993) and case 2 (Loisel and Morel, 2001) waters focus on anisotropy of the underwater light field, described by

126 $\eta$, $N$ and the anisotropy factor $Q$ that relates diffuse upwelling irradiance $E_u^-$ to
127 directional upwelling radiance $L_u^-$. It is found that the directional variations in $f$ and $Q$
128 partly compensate each other, leaving the subsurface remote sensing reflectance $R_{rs}^-$ less
129 sensitive to anisotropy effects than $R^-$ (Morel and Gentili, 1993). Accordingly, semi-
130 analytical models that relate $\omega_b$ directly to $R_{rs}^-$ by means of quadratic coefficients
131 became more popular (Gordon et al., 1988; Lee et al., 1998).
132 Correction for air-water interface and normalization of the resulting $R_{rs}^+$ to zenith
133 illumination and viewing geometry will then result in the normalized water-leaving
134 reflectance $[R_w]_N$ (Gordon et al., 1988; Gordon and Clark, 1981). The calculation of
135 $[R_w]_N$ from at-sensor radiances as well as estimation of the coefficients in semi-
136 analytical models require knowledge of atmospheric and aquatic parameters, which
137 have to be retrieved through iterative procedures (Gordon and Franz, 2008; Morel and
138 Gentili, 1996). Since such procedures are more computationally expensive for case 2
139 than for case 1 waters (Kuchinke et al., 2009a), approximations find wide use in both
140 cases, compromising the potential improvement due to such normalizations.
141

142 # 4 Band arithmetic algorithms

143 *CHL* retrieval band arithmetic algorithms make use of the pigment's primary and
144 secondary absorption maxima at 442 nm and 665 nm, respectively (Bricaud et al.,
145 1995), a reflectance peak around 700 nm due to the minimum sum of absorption of
146 phytoplankton, particulate and dissolved matter and water (Gitelson, 1992; Vasilkov
147 and Kopelevich, 1982; Vos et al., 1986) and its fluorescence emission band at 681 nm
148 (Gower et al., 1999).
149 The primary feature is superimposed by *CDOM* absorption (Bricaud et al., 1981), and
150 therefore widely used in case 1 waters, where *CDOM* and *CHL* correlate as CDOM is a

151 phytoplankton degradation product (Morel and Prieur, 1977). Sensor specific standard
152 algorithms for primary *CHL* absorption bands exist for all medium resolution ocean
153 colour spectrometers (Aiken et al., 1995; Clark, 1997; Morel and Antoine, 2007;
154 Murakami et al., 2006; O'Reilly et al., 1998). They are referred to as OC2, OC3 and
155 OC4 depending on the number of bands used.
156 Using the secondary feature is promoted by weak variations in the spectral properties of
157 all other parameters apart from the increasing absorption by water (Dall'Olmo et al.,
158 2003; Gitelson, 1992; Schalles et al., 1998). Its major limitation is the absence of the
159 feature in oligotrophic and some mesotrophic lakes (Guanter et al., 2010).
160 Fluorescence line height (FLH) and maximum chlorophyll index (MCI) algorithms are
161 linear baseline algorithms for <30 mg/m$^3$ and >100 mg/m$^3$ *CHL* ranges (Gower et al.,
162 2005). They can be applied either with or without atmospheric correction (Binding et
163 al., 2011; Matthews et al., 2010).
164 *TSM* and corresponding particle scattering is best quantified outside the *CHL* or *CDOM*
165 features (Binding et al., 2010). Regression with a single band is possible if an accurate,
166 possibly NIR $L_w$ coupled atmospheric correction is applied (Stumpf et al., 2003). Multi
167 band algorithms are however also used on uncorrected at-sensor radiances (Koponen et
168 al., 2007). The choice of spectral bands in regression algorithms depends on the
169 corresponding concentrations ranges, whereas appropriate wavelengths shift from 550
170 nm towards the red and NIR portions of the spectral range for increasing *TSM* (Wang
171 and Lu, 2010). The increase in absorption of pure water towards the NIR will namely
172 require increasing *TSM* to ensure a sufficient reflectance signal (Ruddick et al., 2006),
173 while less absorbing portions of the spectrum are more suitable for low concentrations.
174 Empirical regression of in situ *TSM* with all eligible bands of a spectroradiometric
175 measurement is a simple way to test this hypothesis (Nechad et al., 2010), and provides

176 the flexibility to derive suitable algorithms even for Landsat TM instruments (Wang et
177 al., 2009; Zhou et al., 2006).
178 *CDOM* retrieval methods are restricted to short visible wavelengths, where absorption
179 of *CDOM* and *CHL* coincide (Babin et al., 2003; Ferreira et al., 2009) and inaccuracies
180 due to NIR derived atmospheric correction are largest (Hu et al., 2000). Accordingly,
181 most band arithmetic approaches relate *CDOM* to a ratio of sensitive bands at <600 nm
182 and normalization bands at >600 nm (Kallio et al., 2001). The choice of suitable sensors
183 is smaller than for the estimation of *CHL* and *TSM*, due to insufficient radiometric
184 accuracy of Hyperion (Giardino et al., 2007) and Landsat Thematic Mapper (Kutser et
185 al., 2005b) in the short wave domain of the spectrum.
186

187 # 5 Spectral inversion algorithms

188 The constitution of spectral inversion algorithms is more heterogeneous than band
189 arithmetic algorithms, with differences in water, interface, atmospheric models and
190 inversion techniques. Spectral inversion algorithms perform a simultaneous retrieval of
191 IOPs and concentrations of the optically active constituents. One of the major
192 weaknesses of these algorithms is related to the appropriate parameterization of the IOP
193 spectral shapes (IOCCG, 2006).
194 Table 1 contains a list of recent studies reporting validation results for spectral inversion
195 algorithms in case 2 waters. NN inversion techniques are dominant, probably due to
196 their improved availability as MERIS level 2 products (Doerffer and Schiller, 2007) and
197 by BEAM plug-ins (Doerffer and Schiller, 2008a; Schroeder et al., 2007b). Other
198 inversion techniques include area minimization (Kutser et al., 2001), matrix inversion
199 (Brando and Dekker, 2003), downhill simplex (Heege and Fischer, 2004), least-squares
200 (Santini et al., 2010), spectral optimization (Kuchinke et al., 2009a) and Levenberg-

Marquardt optimization (Van Der Woerd and Pasterkamp, 2008). Only one application of the SeaDAS semi-analytical algorithms (Carder et al., 1999; Lee et al., 2002; Maritorena et al., 2002) is listed in Table 1. This is however to a large extent due to their focus on retrieving IOPs rather than constituent concentrations.

Most algorithms are used together with specific atmospheric correction modules. The use of standard level 2 reflectance products is only foreseen for two algorithms (Schuchman et al., 2005; Van Der Woerd and Pasterkamp, 2008). The inversion modules match atmospherically corrected $R_{rs}^{+}$ or $R^{-}$ with Hydrolight simulated data (Brando and Dekker, 2003; Doerffer and Schiller, 2007, 2008a; Santini et al., 2010; Van Der Woerd and Pasterkamp, 2008), other numerical (Jerome et al., 1996; Pozdnyakov et al., 2005) or semi-analytical (Heege and Fischer, 2004; Kuchinke et al., 2009a) simulations. Findings from the validation experiments in Table 1 are discussed later.

*Table 1: List of matchup validation experiments with spectral inversion processed spaceborne data. Concentration thresholds in bold letters indicate successful quantitative validation, italic letters indicate successful quantitative falsification, and regular letters indicate missing validation. Expected minimum $R^2$ for validation is 0.4 (CHL, CDOM, tripton) and 0.6 (TSM). Asterisks (*) indicate retrieval of tripton instead of TSM; circles (°) indicate retrieval of inorganic suspended matter instead of TSM; plus signs ($^{+}$) indicate "dissolved organics" [mgC/l] instead of CDOM; carets ($\hat{}$) indicate "colored detrital matter" [$m^{-1}$] instead of CDOM. Concentrations in absorption units are given at 400 nm and, if originally given in another wavelength, converted according to Smith and Baker (1981) with explicitly given spectral exponents (Matthews et al., 2010; Santini et al., 2010) or an approximate 0.017 spectral exponent where not specified (Binding et al., 2011; Giardino et al., 2010; Schroeder et al., 2007b; Van Der Woerd and Pasterkamp, 2008). Algorithm references: [1]Doerffer and Schiller (2007), Moore et al. (1999); [2]Doerffer and Schiller (2008a, b); [3]Schroeder et al. (2007a; 2007b); [4]Pozdnyakov et al. (2005); [5]Brando and Dekker (2003); [6]Heege and Fischer (2004). Strict and relaxed matchups chosen from Cui et al. (2010), Kuchinke et al. (2009b) is omitted due to a lack of absolute in situ concentration values.*

| Experiment | Algorithm | *CHL* [mg/m$^3$] | | *TSM* [g/m$^3$] | | *CDOM* [m$^{-1}$] | |
|---|---|---|---|---|---|---|---|
| | | **max** | **min** | **max** | **min** | **max** | **min** |
| Binding et al. (2011) | NN algal_2[1] | *70.5* | *1.9* | 19.6 | 0.8 | 7.1 | 0.5 |
| Cui et al. (2010) | NN algal_2[1] | **16.1** | **0.7** | *67.8* | *1.5* | 2.0 | 0.7 |
| Minghelli-Roman et al. (2011) | NN algal_2[1] | **9.0** | **0.0** | - | - | - | - |
| Binding et al. (2011) | NN C2R[2] | *70.5* | *1.9* | 19.6 | 0.8 | 7.1 | 0.5 |
| Giardino et al. (2010) | NN C2R[2] | *74.5* | *11.67* | - | - | 4.0 | 1.3 |
| Matthews et al. (2010) | NN C2R[2] | *247.4* | *69.2* | *60.7* | *30.0* | *7.1* | *3.4* |
| Odermatt et al. (2010) | NN C2R[2] | **9.0** | **0.0** | - | - | - | - |
| Schroeder et al. (2007b) | NN FUB[3] | **12.6** | **0.1** | **14.3** | **2.7** | **2.0** | **0.8** |
| Shuchman et al. (2006) | Coupled NN[4] | *2.5* | *0.1* | *2.7°* | *1.3°* | 3.5$^+$ | 0.0$^+$ |
| Giardino et al. (2007) | MIM[5] | **2.2** | **1.3** | **2.1*** | **0.9*** | - | - |
| Odermatt et al. (2008) | MIP[6] | *4.0* | *0.6* | - | - | - | - |
| Santini et al. (2010) | 2 step inversion | 5.0 | 1.8 | 13.0* | 3.0* | 0.8 | 0.1 |
| Van der Woerd and Pasterkamp (2008) | Hydropt | 20.0 | 0.0 | 30.0 | 0.0 | 1.6 | 0.0 |

# 6 Validation experiments

Recent ISI journals (2006-2011) comprise about 50 published papers reporting water constituent retrieval from satellite imagery for optically deep and complex waters, among which about three quarter apply band arithmetic algorithms. Applied selection criteria are the availability of coinciding validation data, concentration ranges and statistical quality measures, namely $R^2$.

## 6.1 Chlorophyll-a retrieval

All recent band arithmetic *CHL* retrieval applications are depicted in Figure 1, with corresponding sensors and concentration ranges. The three previously described major groups are distinguished; green/blue ratios defined for OC algorithms, red-NIR band ratios and further empirical algorithms.

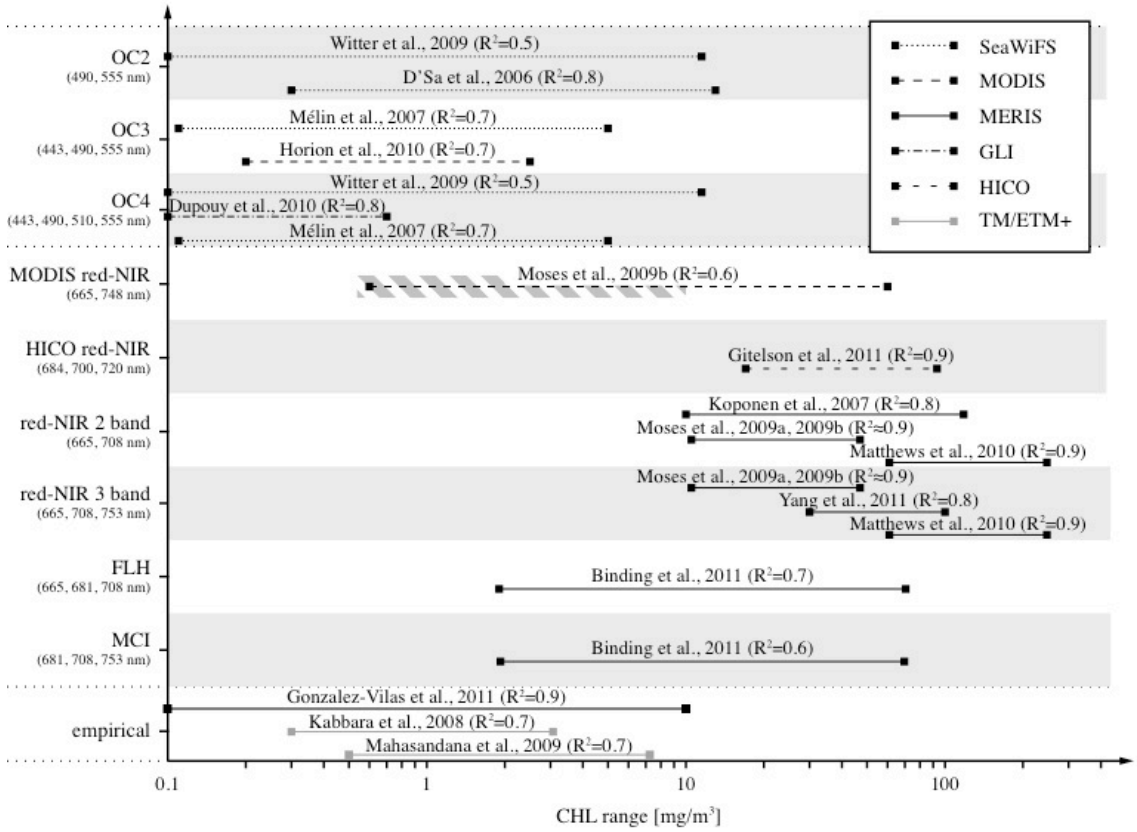


*Figure 1: Overview of recently (2006-2011) published ISI journal papers on the separate retrieval of chl-a from satellite imagery using matchup-validated semi-analytical and empirical algorithms. Hatched areas indicate disputed application ranges. The red-NIR 3 band application by Chen et al. (2011) is omitted since the variation range retrieved from Hyperion (21-27 mg/m$^3$; $R^2$=0.6) is too small to display.*

The OC2-OC4 algorithms are successfully applied to retrieve 0-10 mg/m$^3$ *CHL* in optically complex water. They are however considerably less accurate than red-NIR ratios at high *CHL*, which coincides with theoretical concerns that their use is limited to Open Ocean. This is because independently varying *CDOM* disturb the correlation between such short wavelengths and the primary *CHL* absorption feature. From top to bottom in Figure 1, study areas are Lake Erie (OC2 and OC4), the Mississippi Delta (OC2), Lake Tanganyika (OC3) and the Northern Adriatic Sea (OC3 and OC4), and a lagoon in New Caledonia (OC4). Several of these examples indicate that the observed water optical properties resemble those in case 1 water to some extent. Mélin et al. (2007) mention that two thirds of their observations refer to case 1 water, and Horion et al. (2010) assume explicitly that even Lake Tanganyika is case 1. The data by D'Sa et

al. (2006) follow a shifted but correlated mixture of constituents as found for case 1 water (Morel and Maritorena, 2001), which can be accounted for by regional adjustment as done by Witter et al. (2009). Dupouy et al. (2010) present a turbidity index for the preselection of applicable data points. Atmospheric correction algorithms provide $R_{rs}^{+}$ and $[R_w]_N$ output for application of the OC algorithms (Gordon and Voss, 2004; Gordon and Wang, 1994; Siegel et al., 2000; Stumpf et al., 2003; Toratani et al., 2007). Further OC applications to optically complex waters lack quantitative matchup validation (Gons et al., 2008; Wang et al., 2011; Werdell et al., 2009).

NIR-red algorithms using 2 or 3 bands are validated using MERIS data for up to 250 mg/m$^3$ *CHL* in Zeekoevlei (Matthews et al., 2010), and suitable for the 10-100 mg/m$^3$ interval represented by the Dnieper River, the Sea of Azov, the Gulf of Finland, Lake Dianchi and Kasumigaura, as in vertical order in Figure 1. *CHL* <10 mg/m$^3$ is only observed in Moses et al. (2009a; 2009b). Their calibration data and root mean square errors (RMSEs), as well as previous simulations (Dall'Olmo and Gitelson, 2006) indicate a minimum applicability threshold at 10 mg/m$^3$ *CHL*. Although lower *CHL* is successfully retrieved from field spectroscopy measurements (Gitelson et al., 2009). Enhancement of NIR-red algorithms by *CDOM* and tripton derived coefficients from a look-up-table may even extend the applicable range, but are only validated for waters with high *CHL* (Yang et al., 2011). Advantages in the use of either 2 or 3 bands are inconsistent (Moses et al., 2009a; Moses et al., 2009b). Larger differences in accuracy occur through different atmospheric correction methods. The MERIS bright pixel procedure (Moore et al., 1999) performs considerably better than the C2R atmosphere module (Doerffer and Schiller, 2008b) in Moses et al. (2009b). Other procedures are SCAPE-M (Guanter et al., 2010) for MERIS (Yang et al., 2011) and FLAASH (Cooley et al., 2002) for Hyperion (Chen et al., 2011), which imply the use of either $R_{rs}^{+}$ or $R^{-}$ for *CHL* retrieval. Matthews et al. (2010) demonstrate that NIR-red algorithms can even

286 be used with uncorrected data at the top of atmosphere (TOA). The same applies to
287 MCI, which outperforms FLH, the MERIS Algal_2 and C2R algorithms at the remote
288 measurement of an algae bloom event in the Lake of the Woods (Binding et al., 2011).
289 Accuracy restrictions for low *CHL* are however similar as for the 2 and 3 band NIR-red
290 algorithms as far as RMSE (5.7 and 7.3 $mg/m^3$ for MCI and FLH, respectively) is
291 concerned. FLH was also found inapplicable to oligotrophic water in the Laurentian
292 Lakes, raising concerns over the fluorescence signal to noise ratio under unfavourable
293 atmospheric conditions (Gons et al., 2008).
294 The empirical studies by Kabbara et al. (2008) and Mahasandana et al. (2009) consist of
295 regression models for Landsat-7 ETM+ and Landsat-5 TM. They prove the feasibility
296 of *CHL* estimation with high-resolution sensors, but need parameterization for each
297 single image. In contrast, Gonzalez Vilas et al. (2011) train NNs for preclassified
298 MERIS observations and in situ measured concentrations without the application of an
299 explicit bio-optical model. Their approach achieves high accuracy and temporal stability
300 at the expense of regional restriction.
301 The types of sensors used in the present experiments correlate clearly with the choice of
302 applications; SeaWiFS and MODIS for the OC algorithms and low *CHL* concentrations,
303 MERIS for the retrieval of high *CHL* by means of red-NIR band ratios and Landsat for
304 empirical algorithms. The advantage of MERIS' 681 nm and 708 nm bands over
305 comparable instruments that lack these bands is known (Gitelson et al., 2008; Gower et
306 al., 1999), and demonstrated for MODIS by Moses et al. (2009a). Gitelson et al. (2011)
307 use a set of hyperspectral HICO data to define optical band positions for a 3 band red-
308 NIR algorithm at even higher accuracy.
309 Appropriate atmospheric corrections that preserve the NIR reflectance peak and allow
310 for directional normalization to $[R_w]_N$ are another prerequisite and asset, respectively.
311 The SeaDAS toolbox for SeaWiFS and MODIS offers a large variety in this regard (Hu

et al., 2000; Ruddick et al., 2000; Stumpf et al., 2003; Vidot and Santer, 2005; Wang, 2007), whereas occasional failure in retrieving the NIR peak is reported for MERIS' C2R atmospheric correction module (Guanter et al., 2010; Odermatt et al., 2010).

### 6.2 Suspended sediment retrieval

Recent *TSM* retrieval validation experiments are listed in Figure 2, for increasing central wavelengths of chosen sensors and bands in vertical direction. The convergence in frequently applied methods is not as evident as among the *CHL* algorithms in Figure 1. The advantage of semi-analytical over empirical algorithms is a matter of adaptivity and justification rather than accuracy. Application of semi-analytical algorithms implies a physically sound procedure with defined $R_{rs}^{+}$ from atmospheric correction procedures as mentioned for *CHL* (Moore et al., 1999; Ruddick et al., 2000; Stumpf et al., 2003). Their configuration allows adjustment to other sensors or bands (Van der Woerd and Pasterkamp, 2004), and comparison of atmospheric corrections (Matthews et al., 2010) or reflectance models (Nechad et al., 2010). In contrast, empirical algorithms apart from Petus et al. (2010) and Mélin et al. (2007) are applied to uncorrected at-sensor radiances (Koponen et al., 2007) and physically undefined reflectance quantities (Chen et al., 2009; Wang et al., 2009), leaving them unjustified for applications beyond the data they are derived for. However, empirical algorithms are advantageous for evaluation experiments as with the validation of *TSM* from geostationary MSG-SEVIRI data by means of MODIS *TSM* (Neukermans et al., 2009).

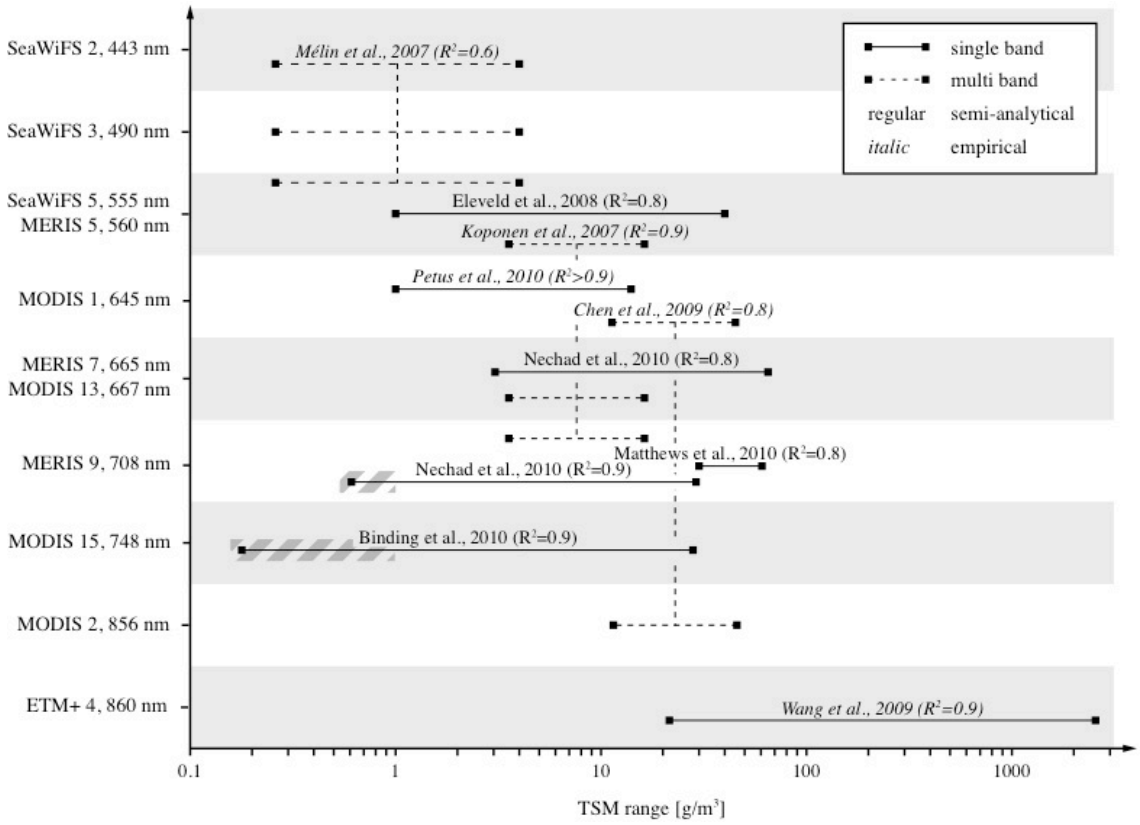


*Figure 2: Overview of recently (2006-2011) published ISI journal papers on the separate retrieval of TSM from satellite imagery by means of matchup-validated semi-analytical and empirical algorithms. Hatched areas indicate disputed application ranges. The retrieval of tripton from MERIS band 10 (754 nm) at $R^2$=0.3 was omitted (Yang et al., 2011).*

An increase in spectral band position with observed *TSM* concentration range is found in Figure 2 as well as in several discussions (Fettweis et al., 2011; Wang and Lu, 2010; Zhang et al., 2010). Maximum sensitivity thresholds are estimated at 30 g/m$^3$ g/m$^3$ for SeaWiFS' 555 nm band (Eleveld et al., 2008) or around 150-200 g/m$^3$ for bands at <650 nm (Fettweis et al., 2011; Wang and Lu, 2010). Only one recent quantitative validation experiment investigates such extreme turbidity, accordingly at 860 nm (Wang et al., 2009). In less turbid water, the accuracy variations for 8 MERIS bands between 620 and 885 nm is only $R^2$=0.89 to 0.93, and lower in absolute values but similar in variation for MODIS (Nechad et al., 2010). Multi band algorithms are recommended for low *TSM* concentrations due to the increasing superimposition by other constituents' optical properties (Nechad et al., 2010). In this regard, Nechad et al. (2010) suggest a 1 g/m$^3$

351 minimum threshold for single band algorithms, while Binding et al. (2010) mention that
352 their RMSE increases to 47% of mean concentrations below 5 g/m$^3$. Matchups in clear
353 Adriatic coastal water, which is in two thirds of all matchups typically oceanic,
354 confirms the challenges in retrieval of low *TSM*, with a relatively low $R^2$ (Mélin et al.,
355 2007).
356
357 **6.3 Dissolved organic matter retrieval**
358 All *CDOM* retrieval band arithmetic algorithms in Figure 3 are from empirical
359 regression (D'Sa and Miller, 2003; Gitelson et al., 1993; Kallio et al., 2001; Kowalczuk
360 et al., 2005), in the case of Yang et al. (2011) by means of bio-optical simulations
361 (Ammenberg et al., 2002). The examples indicate that single band approaches and
362 bands at less than 490 nm are only applicable to extremely high concentrations and
363 correspondingly strong *CDOM* absorption variations as in Zeekoevlei (Matthews et al.,
364 2010). The two best correlations are calculated for band ratios that apply a 442-490 nm
365 band that is sensitive to both *CHL* and *CDOM* variations, and the *CHL*-sensitive 665
366 nm band of MERIS for normalization (Koponen et al., 2007; Matthews et al., 2010). In
367 both cases no atmospheric correction is applied, although *CDOM* in the Gulf of Finland
368 is already much less abundant than in Zeekovlei.
369 Ammenberg et al. (2002) uses the 665 nm band to normalize the 560 nm band rather
370 than the 442-490 nm bands, whereas both the interference with *CHL* absorption and the
371 *CDOM* signal are considerably weaker at 560 nm. The correlation of this ratio with
372 intermediate *CDOM* in Lake Dianchi and Lake Kasumigaura remains however
373 relatively low, in spite of the application of a look-up-table retrieved parameterization
374 (Yang et al., 2011). A recent validation exercise with ALI bands 2 and 3 at similar
375 spectral positions is only qualitative and thus not included in Figure 3 (Kutser et al.,
376 2009). Earlier studies have however demonstrated the potential of this band

377 combination for mapping *CDOM* in inland waters even at high spatial resolution
378 (Kutser et al., 2005a; Kutser et al., 2005b).

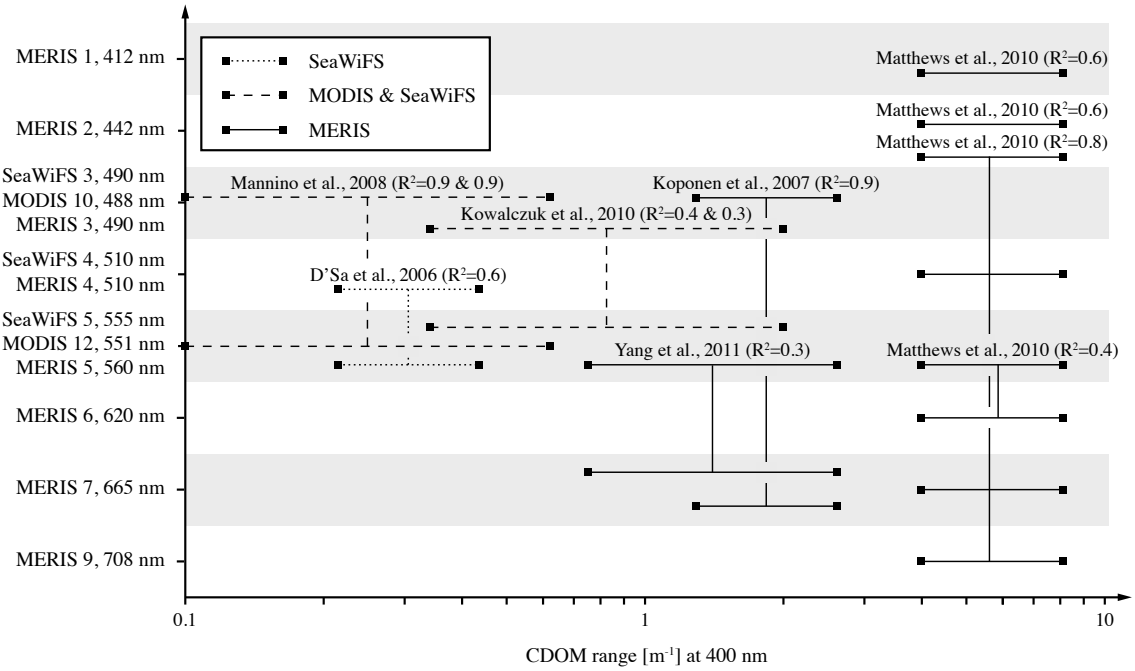


379

380 *Figure 3: Overview of recently (2006-2011) published ISI journal papers on the separate retrieval of*
381 *CDOM from satellite imagery by means of matchup-validated, arithmetic algorithms. Where necessary,*
382 *normalization to 400 nm is done with explicitly mentioned spectral exponents (Smith and Baker, 1981),*
383 *i.e. 0.0157 (Yang et al., 2011), 0.0161 (D'Sa et al., 2006) and 0.0188 (Matthews et al., 2010), or an*
384 *approximate average of 0.0215 (Mannino et al., 2008).*

385

386 The SeaWiFS and MODIS bands ratios recommended by Kowalczuk et al. (2005) and
387 D'Sa and Miller (2003) omit the red-NIR part of the spectrum as previously found for
388 the band arithmetic retrieval of *CHL* with these two instruments. The former was
389 validated with data of the Baltic Sea from both SeaWiFS and MODIS (the latter not
390 shown in Figure 3, $R^2$=0.3) and outperforms the *CDOM* output from SeaDAS semi-
391 analytical algorithms (Carder et al., 1999; Garver and Siegel, 1997; Maritorena et al.,
392 2002) in all cases (Kowalczuk et al., 2010). A SeaWiFS validation in the Mississippi
393 estuary achieves an even higher correlation at lower concentrations (D'Sa et al., 2006).
394 The two validation exercises are also the seasonally most representative ones given that
395 data matchups from several years and seasons are analyzed.

396

397 **6.4 Spectral inversion applications**

398 13 or a quarter of the selected publications in 2006-2011 ISI journals refer to spectral
399 inversion algorithms (Table 1), with several papers on new algorithms where validation
400 is only a subchapter (Santini et al., 2010; Schroeder et al., 2007b; Van Der Woerd and
401 Pasterkamp, 2008). The quantitative content is often less detailed than with band
402 arithmetic algorithms, hindering an estimate of their applicability as shown in Table 1.
403 The MERIS algal_2 product (Doerffer and Schiller, 2007) and *CHL* from C2R and its
404 boreal and eutrophic version (Doerffer and Schiller, 2008a; Koponen et al., 2008) have
405 been applied in several experiments. C2R is successfully validated for low to
406 intermediate concentrations (<16 mg/m$^3$) (Cui et al., 2010; Minghelli-Roman et al.,
407 2011; Odermatt et al., 2010), while C2R and even its eutrophic water version are found
408 unsuitable for high *CHL* concentrations (Binding et al., 2011; Giardino et al., 2010;
409 Matthews et al., 2010). C2R's *CDOM* is found adequate in a eutrophic lagoon in the
410 Baltic Sea, where concurrent *CHL* is strongly underestimated (Giardino et al., 2010). In
411 contrast, *CDOM* in oligotropic perialpine and Finish lakes is underestimated by both
412 C2R and its boreal version while *CHL* is adequate (Koponen et al., 2008; Odermatt et
413 al., 2010). C2R's atmospheric correction failed at retrieving the red-NIR reflectance
414 peak in several examples, while it outperforms other procedures with its accuracy at
415 blue and green wavelengths (Giardino et al., 2010; Odermatt et al., 2010; Odermatt et
416 al., 2008). *TSM* retrieved by the two NN is inapplicable to turbid water (Cui et al., 2010;
417 Matthews et al., 2010), but accurate at about <15-30 g/m$^3$ (Koponen et al., 2008).
418 Validation of the FUB MERIS NN algorithm is successful and thorough at low to
419 intermediate concentrations of all constituents over a wide spatiotemporal range
420 (Schroeder, 2005; Schroeder et al., 2007b). Even lower constituent concentrations are
421 successfully retrieved from a single Hyperion image by means of matrix inversion

(Giardino et al., 2007). All other applications do not meet the requirements for quantitative matchup validation. Ground truth comparisons are limited to spectral fits (Van Der Woerd and Pasterkamp, 2008), frequency distribution (Kuchinke et al., 2009b) and transect comparisons (Santini et al., 2010), or display occasional failure that prevent sufficient correlations (Odermatt et al., 2008; Shuchman et al., 2006).

# 7 Discussion

The assessed quantitative validation experiments using band arithmetic algorithms consist of comparisons of several methods where in situ data are acquired for exactly this validation purpose. They are numerous enough to synthesize several general conclusions based on individual findings and validation sites, e.g. the validity range for red-NIR *CHL* algorithms, the suitability of OC algorithms for low and intermediate *CHL*, the choice of *TSM* retrieval wavelengths according to expected concentrations ranges or the *CHL* variation normalization strategies in *CDOM* retrieval algorithms. A sufficient number of studies with spectral inversion algorithms are only available for the MERIS NN algorithms. Only the algorithm by Schroeder et al. (2007b) has been successfully validated using matchup correlations of all three constituents over several image acquisitions and aquatic regions as given for many band arithmetic algorithms. We presume two main reasons for this difference, namely availability and complexity. The importance of the availability of algorithms is well represented by the frequent use of retrieval algorithms and corresponding atmospheric correction procedures in SeaDAS and BEAM. They lead to the use of OC algorithms, such as the most popular *CHL* retrieval methods based on SeaWiFS and MODIS data, while NN algorithms are evaluated in most experiments using MERIS data. The opposite cases are rare, although not hindered by sensor or data properties. Consequently, the (semi-)operational use of

447 spectral inversion algorithms is mainly limited to their promoters unless other potential
448 users find easier available methods unsuitable, which may again indicate challenging
449 bio-optical conditions, complicating validation.
450 Crucial sensor and data properties are the red-NIR wavebands as used in MERIS, the
451 spatial resolution of Landsat and ALI instruments and the temporal resolution of MSG-
452 SEVIRI. In the first case, the red-NIR *CHL* retrieval experiments with MERIS
453 outnumber and outperform corresponding experiments for most other sensors, rendering
454 MERIS the preferred instrument for estimating *CHL* in meso- to eutrophic waters. In
455 the case of MSG-SEVIRI, TM, ETM+ and ALI, radiometric accuracy, bandwidths and
456 a lack of appropriate preprocessing tools complicate routine use, as established with
457 dedicated ocean color instruments. However, experimental evidence is given that either
458 of those instruments can be used for case 2 water constituent retrieval under certain
459 circumstances. Simpler methods are however mostly empirical, providing rapid access
460 to data and their correlations, but at the cost of being site specific and not expressing
461 any cause-effect relationship.
462 On the opposite side, complexity in constitution, application and validation of spectral
463 inversion procedures is clearly highest. They retrieve several aquatic and possibly
464 atmospheric parameters from a larger number of spectral bands. Failure at any point in
465 the procedure, i.e. the assumption of an inappropriate shape in *CDOM* absorption, may
466 propagate errors in the estimates of other parameters, complicating a coherent validation
467 or falsification. Band arithmetic algorithms on the contrary make use of known
468 relationships between one aquatic parameter and 1-3 spectral bands that are sensitive to
469 an optical property of the sought-after parameter or allow the normalization of other
470 variations. The validation or falsification of such relationships is straightforward and
471 reveals a good estimate of an algorithm's validity range.

For a comparison of the known validity ranges for band arithmetic algorithms (Figure 1 to Figure 3), we apply a scheme that helps to further categorize applications for case 2 waters. Natural variations in each constituent are separated in a low, intermediate and high range. Low *CHL* is referred to as oligotrophic, and ranges up to 3 mg/m$^3$, the integer average from ecological classification schemes (Bukata et al., 1995; Carlson and Simpson, 1996; Chapra and Dobson, 1981; Nürnberg, 1996; Wetzel, 1983). Previous definitions of the second threshold between mesotrophic and eutrophic waters differ from 5.6 to 20 mg/m$^3$ and are supplemented with a hypereutrophic water in some schemes (Table 2). According to these sources and Figure 1 we set the threshold to 10 mg/m$^3$, which approximately limits the applicability of OC and red-NIR algorithms at the top and bottom of their concentration range, respectively. *TSM* thresholds are set at 3 and 30 g/m$^3$ due to the experimental ranges in Figure 2, corresponding water types are referred to as clear, cloudy or turbid. An analogous portioning is carried out for *CDOM* according to Figure 3, allowing the assignment of all collected validation experiments to one or several variation spaces with regard to independent variations in the other two constituents as in Figure 4 (e.g. *TSM* retrieval in clear and cloudy water at given *CHL* and *CDOM* (Binding et al., 2010)).

*Table 2:* Trophic levels for coastal and inland waters and corresponding CHL [mg/m$^3$].

| **Author** | **Oligotrophic** | **Mesotrophic** | **Eutrophic** | **Hypereutr.** |
|---|---|---|---|---|
| Chapra and Dobson (1981) | 0-2.9 | 2.9-5.6 | >5.6 | n.a. |
| Wetzel (1983) | 0.3-4.5 | 3-11 | 3-78 | n.a. |
| Bukata (1995) | 0.8-2.5 | 2.5-6 | 6-18 | >18 |
| Carlson and Simpson (1996) | 0-2.6 | 2.6-20 | 20-56 | >56 |
| Nürnberg (1996) | 0-3.5 | 3.5-9 | 9-25 | >25 |

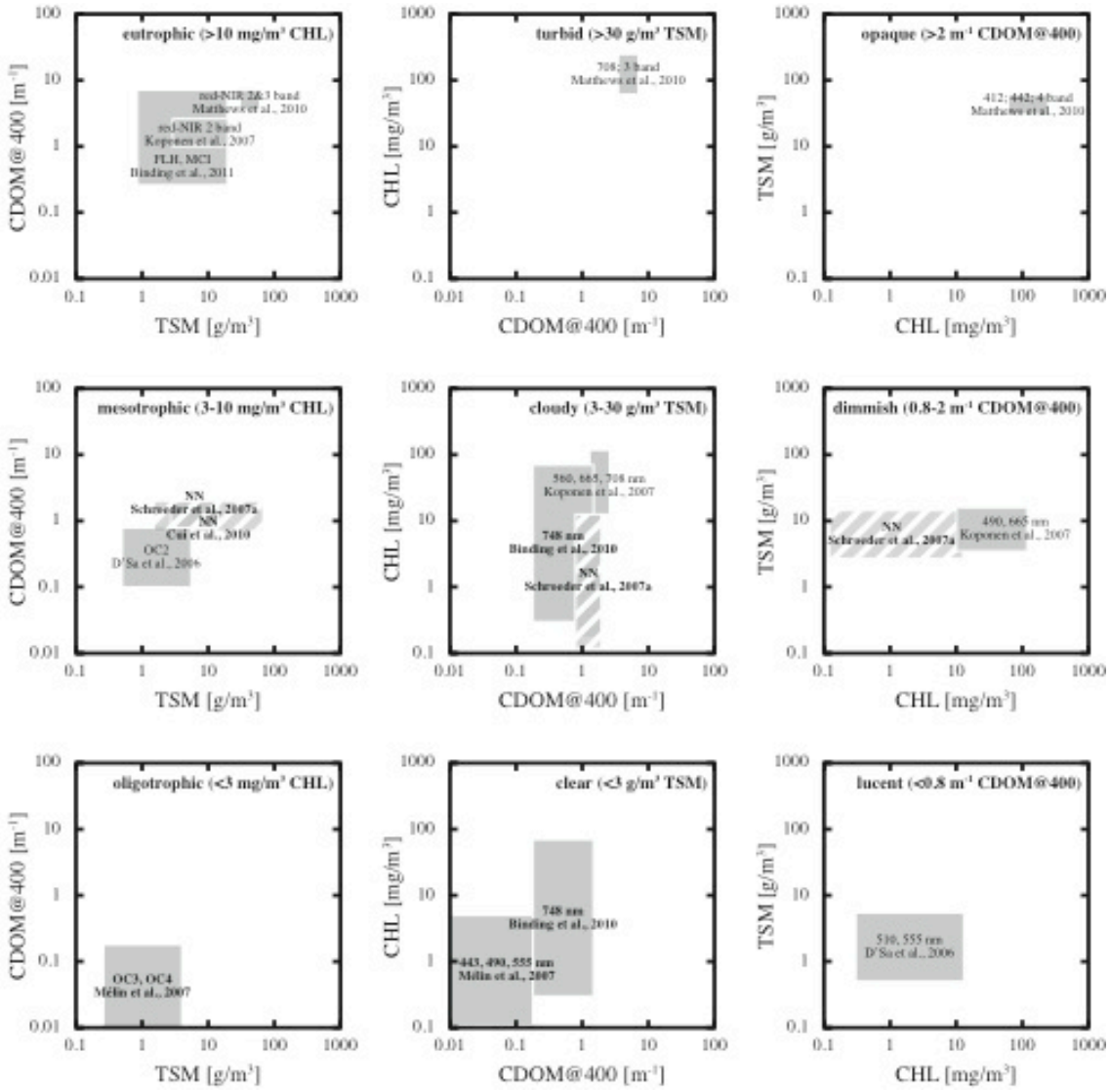


*Figure 4: Case 2 water classes for CHL (left column), TSM (center) and CDOM (right) concentrations, with high to low concentration classes from top to bottom, and the remaining two constituents varying in x- and y-direction of each box. Class names and concentration ranges are titled in each box. Algorithm validation ranges are indicated as boxes and labeled with corresponding retrieval methods or center wavelengths. Bold labels indicate validation experiments with >10 images, hatched areas indicate simultaneous retrieval of all constituents. Reading example: Binding et al. (2011) validate the FLH and MCI algorithms for CHL in eutrophic waters with 0.85-19.60 g/m³ TSM and 0.26-7.14 m⁻¹ CDOM.*

Published validation experiments as used in Figure 1 to Figure 3 are depicted in Figure 4 if variation ranges of all three constituents are given, even if only individual constituents are retrieved. Only two spectral inversion experiments from Table 1 can be positioned. Schroeder et al. (2007b) present simultaneous retrieval of all parameters at an accuracy that is comparable to corresponding band ratio validations, while only *CHL*

507 is retrieved accurately in Cui et al. (2010), but variations in *TSM* and *CDOM* are also
508 given. The *CHL* retrieval column in Figure 4 shows the suitability of red-NIR
509 algorithms for eutrophic water, and the potential of OC algorithms for oligo- to
510 mesotrophic waters at relatively low *TSM* and *CDOM* variations. Several different
511 algorithms retrieve *TSM* accurately, but the relationship between sensitive wavelength
512 and concentration range (Figure 2) is no more visible. Relatively few experiments are
513 assigned to turbid water, probably because measuring in situ *TSM* is much less of an
514 effort than additional *CHL* and *CDOM*. The proof of successful *CDOM* retrieval is
515 however generally scarce, similar as with low *CHL* concentrations.
516 The directional reflectance properties of water are often neglected. Spectral inversion
517 algorithms that make use of directional radiative transfer simulations are the most
518 adequate solution, as they can account for all influencing parameters assuming a given
519 $\tilde{\beta}(\psi)$ (Doerffer and Schiller, 2008a; Giardino et al., 2007; Van Der Woerd and
520 Pasterkamp, 2008). Regarding classical analytical approaches, directional effects are
521 parameterized using coefficients (e.g. $f$, $Q$) that vary with constituent concentrations
522 (Morel and Gentili, 1991, 1993). Their estimation requires iterative optimization, which
523 needs an extension for band arithmetic analysis (Yang et al., 2011). More recent
524 analytical models are even parameterized with a specific geometry (Albert and Mobley,
525 2003; Park and Ruddick, 2005). A corresponding application example is given in
526 Nechad et al. (2010), where the retrieval of *TSM* from cloudy water using a classical
527 model (Gordon et al., 1988) is surprisingly better than a directional model (Park and
528 Ruddick, 2005). Nonetheless, an improvement is expected especially for water with less
529 particle scattering, i.e. higher $\eta$ and lower $N$, and thus with higher anisotropy.
530 Atmospheric correction procedures that provide an accurate $[R_w]_N$ e.g. through iterative
531 procedures are thereby eligible alternatives to more extensively parameterized
532 reflectance models.

The prominence of band-ratio algorithms for the individual retrieval of CHL in case 2 waters reported in this study, warrants however a note of caution. It has been suggested that changes on phytoplankton assemblages, as due to climate change, may shift phytoplankton composition in response to altered environmental forcing (e.g. Montes-Hugo et al., 2008). This process might uncouple *CDOM* and *TSM* concentrations from phytoplankton stocks and lead to further uncertainty in the retrieval of individual constituents, which is usually the case when using empirical algorithms, as opposed to the consolidated retrieval by inversion algorithms (Dierssen, 2010).

Extending from the intercomparison of algorithms performance based on synthetic and in situ data sets (IOCCG, 2006), a series of intercomparison and benchmark exercises including application to satellite imagery and matchup analysis is recommended to shed light on the comparability of water constituent retrieval algorithms and identify their applicability constraints in the near future.

## Acknowledgements

We appreciate early comments and discussions on this work, in particular by Young-Je Park, Arnold Dekker, Els Knaeps, Dries Raymaekers and Viacheslav Kiselev. This work was partly funded by CSIRO's Wealth from Oceans Flagship and by NASA LCLUC program to AAG.

## References

Aiken, J., Moore, G.F., Trees, C.C., Hooker, S.B., & Clark, D.K. (1995). The SeaWiFS CZCS-type pigment algorithm. In: *SeaWiFS Technical Report Series*, *29* (38 p.), S.B. Hooker & E.R. Firestone (Eds.), Goddard Space Flight Center

557 Albert, A., & Mobley, C.D. (2003). An analytical model for subsurface irradiance and
558 remote sensing reflectance in deep and shallow case-2 water. *Optics Express,* 11/22,
559 2873-2890
560 Ammenberg, P., Flink, P., Lindell, T., Pierson, D.C., & Strombeck, N. (2002). Bio-
561 optical modelling combined with remote sensing to assess water quality. *International*
562 *Journal of Remote Sensing,* 23/8, 1621
563 Austin, R.W., & Petzold, T.J. (1981). Water Colour Measurements. In J. Gower (Ed.),
564 *Oceanography from Space* (pp. 239-256). New York: Plenum
565 Babin, M., Stramski, D., Ferrari, G.M., Claustre, H., Bricaud, A., Obolensky, G., &
566 Hoepffner, N. (2003). Variations in the light absorption coefficients of phytoplankton,
567 nonalgal particles, and dissolved organic matter in coastal waters around Europe. *J.*
568 *Geophys. Res.,* 108/C7, 3211
569 Belzile, C., Vincent, W.F., Howard-Williams, C., Hawes, I., James, M.R., Kumagai,
570 M., & Roesler, C.S. (2004). Relationships between spectral optical properties and
571 optically active substances in a clear oligotrophic lake. *Water Resour. Res.,* 40/,
572 W12512
573 Binding, C.E., Greenberg, T.A., Jerome, J.H., Bukata, R.P., & Letourneau, G. (2011).
574 An assessment of MERIS algal products during an intense bloom in Lake of the Woods.
575 *Journal of Plankton Research,* 33/5, 793-806
576 Binding, C.E., Jerome, J.H., Bukata, R.P., & Booty, W.G. (2010). Suspended
577 particulate matter in Lake Erie derived from MODIS aquatic colour imagery.
578 *International Journal of Remote Sensing,* 31/19, 5239 - 5255
579 Brando, V.E., & Dekker, A.G. (2003). Satellite hyperspectral remote sensing for
580 estimating estuarine and coastal water quality. *IEEE Transactions on Geoscience and*
581 *Remote Sensing,* 41/6, 1378-1387

582 Bricaud, A., Morel, A., & Prieur, L. (1981). Absorption by dissolved organic matter of
583 the sea (yellow substance) in the UV and visible domains. *Limnology and*
584 *Oceanography,* 26/1, 43-53
585 Bricaud, A., Roesler, C., & Zaneveld, J.R.V. (1995). In Situ Methods for Measuring the
586 Inherent Optical Properties of Ocean Waters. *Limnology and Oceanography,* 40/2, 393-
587 410
588 Bukata, R.P., Jerome, J.H., Kondratyev, K.Y., & Pozdnyakov, D.V. (1995). *Optical*
589 *Properties and Remote Sensing of Inland and Coastal Waters*: CRS Press, USA
590 Bulgarelli, B., Kiselev, V., & Roberti, L. (1999). Radiative transfer in the atmosphere-
591 ocean system: The finite-element method. *Appl. Opt.,* 38/9, 1530-1542
592 Carder, K.L., Chen, F.R., Lee, Z.P., Hawes, S.K., & Kamykowski, D. (1999).
593 Semianalytic Moderate-Resolution Imaging Spectrometer algorithms for chlorophyll a
594 and absorption with bio-optical domains based on nitrate-depletion temperatures. *J.*
595 *Geophys. Res.,* 104/C3, 5403-5421
596 Carlson, R.E., & Simpson, J. (1996). A Coordinator's Guide to Volunteer Lake
597 Monitoring Methods. (96 p.), North American Lake Management Society
598 Chami, M., McKee, D., Leymarie, E., & Khomenko, G. (2006). Influence of the angular
599 shape of the volume-scattering function and multiple scattering on remote sensing
600 reflectance. *Appl. Opt.,* 45/36, 9210-9220
601 Chapra, S.C., & Dobson, H.F.H. (1981). Quantification of the Lake Trophic Typologies
602 of Naumann (Surface Quality) and Thienemann (Oxygen) with Special Reference to the
603 Great Lakes. *Journal of Great Lakes Research,* 7/2, 182-193
604 Chen, S., Fang, L., Li, H., Chen, W., & Huang, W. (2011). Evaluation of a three-band
605 model for estimating chlorophyll-a concentration in tidal reaches of the Pearl River
606 Estuary, China. *ISPRS Journal of Photogrammetry and Remote Sensing,* 66/3, 356-364

607 Chen, S., Huang, W., Wang, H., & Li, D. (2009). Remote sensing assessment of
608 sediment re-suspension during Hurricane Frances in Apalachicola Bay, USA. *Remote*
609 *Sensing of Environment,* 113/12, 2670-2681
610 Cheng Feng, L., Yun Mei, L., Yong, Z., Deyong, S., & Bin, Y. (2009). Validation of a
611 Quasi-Analytical Algorithm for Highly Turbid Eutrophic Water of Meiliang Bay in
612 Taihu Lake, China. *Geoscience and Remote Sensing, IEEE Transactions on,* 47/8,
613 2492-2500
614 Clark, D. (1997). Bio-optical algorithms - Case 1 waters. In: *MODIS algorithm*
615 *theoretical basis document*, *Version 1.2* (50 p.), National Oceanic and Atmospheric
616 Administration
617 Cooley, T., Anderson, G.P., Felde, G.W., Hoke, M.L., Ratkowski, A.J., Chetwynd, J.H.,
618 Gardner, J.A., Adler-Golden, S.M., Matthew, M.W., Berk, A., Bernstein, L.S., Acharya,
619 P.K., Miller, D., & Lewis, P. (2002). FLAASH, a Modtran4-based atmospheric
620 correction algorithm, its application and validation. *Proc. Geoscience and Remote*
621 *Sensing Symposium, 2002. IGARSS '02. 2002 IEEE International*, 1414-1418 vol.1413
622 Cui, T., Zhang, J., Groom, S., Sun, L., Smyth, T., & Sathyendranath, S. (2010).
623 Validation of MERIS ocean-color products in the Bohai Sea: A case study for turbid
624 coastal waters. *Remote Sensing of Environment,* 114/10, 2326-2336
625 D'Sa, E.J., & Miller, R.L. (2003). Bio-optical properties in waters influenced by the
626 Mississippi River during low flow conditions. *Remote Sensing of Environment,* 84/4,
627 538
628 D'Sa, E.J., Miller, R.L., & Del Castillo, C. (2006). Bio-optical properties and ocean
629 color algorithms for coastal waters influenced by the Mississippi River during a cold
630 front. *Appl. Opt.,* 45/28, 7410-7428
631 Dall'Olmo, G., & Gitelson, A.A. (2006). Effect of bio-optical parameter variability and
632 uncertainties in reflectance measurements on the remote estimation of chlorophyll-a

633 concentration in turbid productive waters: modeling results. *Applied Optics,* 45/15,
634 3577-3593
635 Dall'Olmo, G., Gitelson, A.A., & Rundquist, D.C. (2003). Towards a unified approach
636 for remote estimation of chlorophyll-a in both terrestrial vegetation and turbid
637 productive waters. *Geophys. Res. Lett.,* 30/18, 1938
638 Dekker, A.G., Malthus, T.J., & Hoogenboom, H.J. (1995). The Remote Sensing of
639 Inland Water Quality. In F.M. Danson & S.E. Plummer (Eds.), *Advances in*
640 *Environmental Remote Sensing* (pp. 123-142): John Wiley & Sons Ltd
641 Dekker, A.G., & Peters, S.W.M. (1993). Use of the Thematic Mapper for the
642 analysis of eutrophic lakes: A case study in the Netherlands. *International Journal*
643 *of Remote Sensing,* 14/5, 799-821
644 Dierssen, H.M. (2010). Perspectives on empirical approaches for ocean color remote
645 sensing of chlorophyll in a changing climate. *Proceedings of the National Academy of*
646 *Sciences,* 107/40, 17073-17078
647 Doerffer, R., & Schiller, H. (2007). The MERIS case 2 water algorithm. *International*
648 *Journal of Remote Sensing,* 28/3, 517-535
649 Doerffer, R., & Schiller, H. (2008a). MERIS lake water algorithm for BEAM. In:
650 *BEAM Algorithm Technical Basis Document* (17 p.), GKSS Forschungszentrum,
651 Geesthacht, Germany
652 Doerffer, R., & Schiller, H. (2008b). MERIS regional coastal and lake case 2 water
653 project atmospheric correction. In: *BEAM Algorithm Technical Basis Document* (42 p.),
654 GKSS Forschungszentrum, Geesthacht, Germany
655 Dupouy, C., Neveux, J., Ouillon, S., Frouin, R., Murakami, H., Hochard, S., & Dirberg,
656 G. (2010). Inherent optical properties and satellite retrieval of chlorophyll concentration
657 in the lagoon and open ocean waters of New Caledonia. *Marine Pollution Bulletin,*
658 61/7-12, 503-518

659 Eleveld, M.A., Pasterkamp, R., van der Woerd, H.J., & Pietrzak, J.D. (2008). Remotely
660 sensed seasonality in the spatial distribution of sea-surface suspended particulate matter
661 in the southern North Sea. *Estuarine, Coastal and Shelf Science,* 80/1, 103-113
662 Ferreira, A.b., Garcia, V.M.T., & Garcia, C.A.E. (2009). Light absorption by
663 phytoplankton, non-algal particles and dissolved organic matter at the Patagonia shelf-
664 break in spring and summer. *Deep Sea Research Part I: Oceanographic Research*
665 *Papers,* 56/12, 2162-2174
666 Fettweis, M., Baeye, M., Francken, F., Lauwaert, B., Van den Eynde, D., Van Lancker,
667 V., Martens, C., & Michielsen, T. (2011). Monitoring the effects of disposal of fine
668 sediments from maintenance dredging on suspended particulate matter concentration in
669 the Belgian nearshore area (southern North Sea). *Marine Pollution Bulletin,* 62/2, 258-
670 269
671 Fournier, G.R., & Forand, J.L. (1994). *Analytic phase function for ocean water*. Bergen,
672 Norway
673 Fournier, G.R., & Jonasz, M. (1999). Computer-based underwater imaging analysis,
674 Denver, CO, USA, 62-70
675 Freda, W., Król, T., Martynov, O.V., Shybanov, E.B., & Hapter, R. (2007).
676 Measurements of Scattering Function of sea water in Southern Baltic. *The European*
677 *Physical Journal - Special Topics,* 144/1, 147-154
678 Freda, W., & Piskozub, J. (2007). Improved method of Fournier-Forand marine phase
679 function parameterization. *Opt. Express,* 15/20, 12763-12768
680 Garver, S.A., & Siegel, D.A. (1997). Inherent optical property inversion of ocean color
681 spectra and its biogeochemical interpretation 1. Time series from the Sargasso Sea. *J.*
682 *Geophys. Res.,* 102/C8, 18607-18625

683 Giardino, C., Brando, V.E., Dekker, A.G., Strömbeck, N., & Candiani, G. (2007).
684 Assessment of water quality in Lake Garda (Italy) using Hyperion. *Remote Sensing of*
685 *Environment,* 109/2, 183-195
686 Giardino, C., Bresciani, M., Pilkaityte, R., Bartoli, M., & Razinkovas, A. (2010). In situ
687 measurements and satellite remote sensing of case 2 waters: first results from the
688 Curonian Lagoon *Oceanologia,* 52/2, 197-210
689 Gitelson, A. (1992). The peak near 700 nm on radiance spectra of algae and water:
690 relationships of its magnitude and position with chlorophyll concentration. *International*
691 *Journal of Remote Sensing,* 13/17, 3367 - 3373
692 Gitelson, A., Gao, B.-C., Li, R.-R., Berdnikov, S., & Saprygin, V. (2011). Estimation of
693 chlorophyll-a concentration in productive turbid waters using a Hyperspectral Imager
694 for the Coastal Ocean: The Azov Sea case study. *Environmental Research Letters,*
695 6/024023, 6
696 Gitelson, A., Garbuzov, G., Szilagyi, F., Mittenzwey, K.H., Karnieli, A., & Kaiser, A.
697 (1993). Quantitative remote sensing methods for real-time monitoring of inland waters
698 quality. *International Journal of Remote Sensing,* 14/7, 1269-1295
699 Gitelson, A., Gurlin, D., Moses, W.J., & Barrow, T. (2009). A bio-optical algorithm for
700 the remote estimation of the chlorophyll- a concentration in case 2 waters.
701 *Environmental Research Letters,* 4/045003, 5
702 Gitelson, A.A., Dall'Olmo, G., Moses, W., Rundquist, D.C., Barrow, T., Fisher, T.R.,
703 Gurlin, D., & Holz, J. (2008). A simple semi-analytical model for remote estimation of
704 chlorophyll-a in turbid waters: Validation. *Remote Sensing of Environment,* 112/9,
705 3582-3593
706 Gitelson, A.A., Schalles, J.F., & Hladik, C.M. (2007). Remote chlorophyll-a retrieval in
707 turbid, productive estuaries: Chesapeake Bay case study. *Remote Sensing of*
708 *Environment,* 109/4, 464-472

709 Gons, H.J., Auer, M.T., & Effler, S.W. (2008). MERIS satellite chlorophyll mapping of
710 oligotrophic and eutrophic waters in the Laurentian Great Lakes. *Remote Sensing of*
711 *Environment,* 112/11, 4098-4106
712 Gonzalez Vilas, L., Spyrakos, E., & Torres Palenzuela, J.M. (2011). Neural network
713 estimation of chlorophyll a from MERIS full resolution data for the coastal waters of
714 Galician rias (NW Spain). *Remote Sensing of Environment,* 115/2, 524-535
715 Gordon, H.R. (1989). Dependence of the Diffuse Reflectance of Natural Waters on the
716 Sun Angle. *Limnology and Oceanography,* 34/8, 1484-1489
717 Gordon, H.R. (1993). Sensitivity of radiative transfer to small-angle scattering in the
718 ocean: Quantitative assessment. *Applied Optics,* 32/36, 7505-7511
719 Gordon, H.R., & Brown, O.B. (1973). Irradiance Reflectivity of a Flat Ocean as a
720 Function of Its Optical Properties. *Appl. Opt.,* 12/7, 1549-1551
721 Gordon, H.R., Brown, O.B., Evans, R.H., Brown, J.W., Smith, R.C., Baker, K.S., &
722 Clark, D.K. (1988). A semianalytic radiance model of ocean color. *J. Geophys. Res.,*
723 93/D9, 10909-10924
724 Gordon, H.R., Brown, O.B., & Jacobs, M.M. (1975). Computed Relationships Between
725 the Inherent and Apparent Optical Properties of a Flat Homogeneous Ocean. *Appl. Opt.,*
726 14/2, 417-427
727 Gordon, H.R., & Clark, D.K. (1981). Clear water radiances for atmospheric correction
728 of coastal zone color scanner imagery. *Appl. Opt.,* 20/24, 4175-4180
729 Gordon, H.R., & Franz, B.A. (2008). Remote sensing of ocean color: Assessment of the
730 water-leaving radiance bidirectional effects on the atmospheric diffuse transmittance for
731 SeaWiFS and MODIS intercomparisons. *Remote Sensing of Environment,* 112/5, 2677-
732 2685
733 Gordon, H.R., & Voss, K.J. (2004). MODIS Normalized Water-leaving Radiance. In:
734 *MODIS algorithm theoretical basis documents*, *MOD-18* (125 p.)

735 Gordon, H.R., & Wang, M. (1994). Retrieval of water-leaving radiance and aerosol
736 optical thickness over the oceans with SeaWiFS: a preliminary algorithm. *Applied*
737 *Optics,* 33/, 443-452
738 Gower, J., King, S., Borstad, G., & Brown, L. (2005). Detection of intense plankton
739 blooms using the 709 nm band of the MERIS imaging spectrometer. *International*
740 *Journal of Remote Sensing,* 26/9, 2005
741 Gower, J.F.R., Doerffer, R., & Borstad, G.A. (1999). Interpretation of the 685nm peak
742 in water-leaving radiance spectra in terms of fluorescence, absorption and scattering,
743 and its observation by MERIS. *International Journal of Remote Sensing,* 20/9, 1771-
744 1786
745 Guanter, L., Ruiz-Verdu, A., Odermatt, D., Giardino, C., Simis, S., Estelles, V., Heege,
746 T., Dominguez-Gomez, J.A., & Moreno, J. (2010). Atmospheric correction of
747 ENVISAT/MERIS data over inland waters: Validation for European lakes. *Remote*
748 *Sensing of Environment,* 114/3, 467-480
749 Haltrin, V.I. (2002). One-Parameter Two-Term Henyey-Greenstein Phase Function for
750 Light Scattering in Seawater. *Appl. Opt.,* 41/6, 1022-1028
751 Heege, T., & Fischer, J. (2004). Mapping of water constituents in Lake Constance using
752 multispectral airborne scanner data and a physically based processing scheme.
753 *Canadian Journal of Remote Sensing,* 30/1, 77-86
754 Horion, S., Bergamino, N., Stenuite, S., Descy, J.P., Plisnier, P.D., Loiselle, S.A., &
755 Cornet, Y. (2010). Optimized extraction of daily bio-optical time series derived from
756 MODIS/Aqua imagery for Lake Tanganyika, Africa. *Remote Sensing of Environment,*
757 114/4, 781-791
758 Hu, C., Carder, K.L., & Muller-Karger, F.E. (2000). Atmospheric correction of
759 SeaWiFS imagery over turbid coastal waters: A practical method. *Remote Sensing of*
760 *Environment,* 74/2, 195

761 Iluz, D., Yacobi, Y.Z., & Gitelson, A.A. (2003). Adaptation of an algorithm for
762 chlorophyll-a estimation by optical data in the oligotrophic Gulf of Eilat. *International*
763 *Journal of Remote Sensing,* 24/5, 1157
764 IOCCG (2006). Remote Sensing of Inherent Optical Properties: Fundamentals, Tests of
765 Algorithms, and Applications. In: *Reports of the International Ocean-Colour*
766 *Coordinating Group* (122 p.), Z.P. Lee (Ed.), IOCCG
767 IOCCG (2009). Partition of the Ocean into Ecological Provinces: Role of Ocean-Colour
768 Radiometry. In: *Reports of the International Ocean-Colour Coordinating Group* (98
769 p.), M. Dowell & T. Platt (Eds.), IOCCG
770 Jerome, J.H., Bukata, R.P., & Miller, J.R. (1996). Remote sensing reflectance and its
771 relationship to optical properties of natural waters. *International Journal of Remote*
772 *Sensing,* 17/16, 3135-3155
773 Jin, Z., & Stamnes, K. (1994). Radiative transfer in nonuniformly refracting layered
774 media: Atmosphere-ocean system. *Appl. Opt.,* 33/, 431-442
775 Kabbara, N., Benkhelil, J., Awad, M., & Barale, V. (2008). Monitoring water quality in
776 the coastal area of Tripoli (Lebanon) using high-resolution satellite data. *ISPRS Journal*
777 *of Photogrammetry and Remote Sensing,* 63/5, 488-495
778 Kallio, K., Kutser, T., Hannonen, T., Koponen, S., Pulliainen, J., Vepsalainen, J., &
779 Pyhalahti, T. (2001). Retrieval of water quality from airborne imaging spectrometry of
780 various lake types in different seasons. *The Science of The Total Environment,* 268/1-3,
781 59-77
782 Kirk, J.T.O. (1991). Volume scattering function, average cosines, and the underwater
783 light field. *Limnology and Oceanography,* 36/3, 455-467
784 Koponen, S., Attila, J., Pulliainen, J., Kallio, K., Pyh‰lahti, T., Lindfors, A., Rasmus,
785 K., & Hallikainen, M. (2007). A case study of airborne and satellite remote sensing of a
786 spring bloom event in the Gulf of Finland. *Continental Shelf Research,* 27/2, 228-244

787 Koponen, S., Ruiz-Verdu, A., Heege, T., Heblinski, J., Sorensen, K., Kallio, K.,
788 Pyhalahti, T., Doerffer, R., Brockmann, C., & Peters, M. (2008). Development of
789 MERIS lake water algorithms. In: *ESA Validation Report* (65 p.)
790 Kostadinov, T.S., Siegel, D.A., Maritorena, S., & Guillocheau, N. (2007). Ocean color
791 observations and modeling for an optically complex site: Santa Barbara Channel,
792 California, USA. *J. Geophys. Res.,* 112/C7, C07011
793 Kowalczuk, P., Darecki, M., Zablocka, M., & Gorecka, I. (2010). Validation of
794 empirical and semi-analytical remote sensing algorithms for estimating absorption by
795 Coloured Dissolved Organic Matter in the Baltic Sea from SeaWiFS and MODIS
796 imagery. *Oceanologia,* 52/2, 171-196
797 Kowalczuk, P., Olszewski, J., Darecki, M., & Kaczmarek, S. (2005). Empirical
798 relationships between coloured dissolved organic matter (CDOM) absorption and
799 apparent optical properties in Baltic Sea waters. *International Journal of Remote*
800 *Sensing,* 26/2, 345-370
801 Kuchinke, C.P., Gordon, H.R., & Franz, B.A. (2009a). Spectral optimization for
802 constituent retrieval in Case 2 waters I: Implementation and performance. *Remote*
803 *Sensing of Environment,* 113/3, 571-587
804 Kuchinke, C.P., Gordon, H.R., Harding Jr, L.W., & Voss, K.J. (2009b). Spectral
805 optimization for constituent retrieval in Case 2 waters II: Validation study in the
806 Chesapeake Bay. *Remote Sensing of Environment,* 113/3, 610-621
807 Kutser, T., Herlevi, A., Kallio, K., & Arst, H. (2001). A hyperspectral model for
808 interpretation of passive optical remote sensing data from turbid lakes. *The Science of*
809 *The Total Environment,* 268/1-3, 47
810 Kutser, T., Paavel, B., Metsamaa, L., & Vahtmäe, E. (2009). Mapping coloured
811 dissolved organic matter concentration in coastal waters. *International Journal of*
812 *Remote Sensing,* 30/22, 5843 - 5849

813 Kutser, T., Pierson, D.C., Kallio, K.Y., Reinart, A., & Sobek, S. (2005a). Mapping lake
814 CDOM by satellite remote sensing. *Remote Sensing of Environment,* 94/4, 535
815 Kutser, T., Pierson, D.C., Tranvik, L., Reinart, A., Sobek, S., & Kallio, K.Y. (2005b).
816 Using satellite remote sensing to estimate the colored dissolved organic matter
817 absorption coefficient in lakes. *Ecosystems,* 8/6, 709
818 Lee, M.E., & Lewis, M.R. (2003). A New Method for the Measurement of the Optical
819 Volume Scattering Function in the Upper Ocean. *Journal of Atmospheric and Oceanic*
820 *Technology,* 20/4, 563-571
821 Lee, Z., Carder, K.L., & Arnone, R.A. (2002). Deriving Inherent Optical Properties
822 from Water Color: a Multiband Quasi-Analytical Algorithm for Optically Deep Waters.
823 *Appl. Opt.,* 41/27, 5755-5772
824 Lee, Z., Carder, K.L., Mobley, C.D., Steward, R.G., & Patch, J.S. (1998). Hyperspectral
825 Remote Sensing for Shallow Waters. I. A Semianalytical Model. *Appl. Opt.,* 37/27,
826 6329-6338
827 Loisel, H., & Morel, A. (2001). Non-isotropy of the upward radiance field in typical
828 coastal (Case 2) waters. *International Journal of Remote Sensing,* 22/2, 275 - 295
829 Mahasandana, S., Tripathi, N.K., & Honda, K. (2009). Sea surface multispectral index
830 model for estimating chlorophyll a concentration of productive coastal waters in
831 Thailand. *Canadian Journal of Remote Sensing,* 35/3, 287-296
832 Mannino, A., Russ, M.E., & Hooker, S.B. (2008). Algorithm development and
833 validation for satellite-derived distributions of DOC and CDOM in the U.S. Middle
834 Atlantic Bight. *J. Geophys. Res.,* 113/C7, C07051
835 Maritorena, S., Siegel, D.A., & Peterson, A.R. (2002). Optimization of a semianalytical
836 ocean color model for global-scale applications. *Appl. Opt.,* 41/15, 2705-2714

837 Matthews, M.W. (2011). A current review of empirical procedures of remote sensing in
838 inland and near-coastal transitional waters. *International Journal of Remote Sensing,*
839 32/21, 6855-6899
840 Matthews, M.W., Bernard, S., & Winter, K. (2010). Remote sensing of cyanobacteria-
841 dominant algal blooms and water quality parameters in Zeekoevlei, a small
842 hypertrophic lake, using MERIS. *Remote Sensing of Environment,* 114/9, 2070-2087
843 McClain, C.R. (2009). A Decade of Satellite Ocean Color Observations. *Annual Review*
844 *of Marine Science,* 1/1, 19-42
845 Mélin, F., Zibordi, G., & Berthon, J.-F. (2007). Assessment of satellite ocean color
846 products at a coastal site. *Remote Sensing of Environment,* 110/2, 192-215
847 Minghelli-Roman, A., Laugier, T., Polidori, L., Mathieu, S., Loubersac, L., & Gouton,
848 P. (2011). Satellite survey of seasonal trophic status and occasional anoxic 'malaigue'
849 crises in the Thau lagoon using MERIS images. *International Journal of Remote*
850 *Sensing,* 32/4, 909-923
851 Mobley, C.D. (1989). A Numerical Model for the Computation of Radiance
852 Distributions in Natural Waters with Wind-Roughened Surfaces. *Limnology and*
853 *Oceanography,* 34/8, 1473-1483
854 Mobley, C.D., Gentili, B., Gordon, H.R., Jin, Z., Kattawar, G.W., Morel, A.,
855 Reinersman, P., Stamnes, K., & Stavn, R.H. (1993). Comparison of numerical models
856 for computing underwater light fields. *Appl. Opt.,* 32/36, 7484-7504
857 Mobley, C.D., Sundman, L.K., & Boss, E. (2002). Phase Function Effects on Oceanic
858 Light Fields. *Appl. Opt.,* 41/6, 1035-1050
859 Montes-Hugo, M.A., Vernet, M., Smith, R., & Carder, K. (2008). Phytoplankton size-
860 structure on the western shelf of the Antarctic Peninsula: a remote-sensing approach.
861 *Int. J. Remote Sens.,* 29/3, 801-829

862 Moore, G.F., Aiken, J., & Lavender, S.J. (1999). The atmospheric correction of water
863 colour and the quantitative retrieval of suspended particulate matter in Case II waters:
864 application to MERIS. *International Journal of Remote Sensing,* 20/9, 1713 - 1733
865 Moore, T.S., Campbell, J.W., & Dowell, M.D. (2009). A class-based approach to
866 characterizing and mapping the uncertainty of the MODIS ocean chlorophyll product.
867 *Remote Sensing of Environment,* 113/11, 2424-2430
868 Morel, A. (1974). Optical properties of pure water and pure sea water. In N.G. Jerlov &
869 E.S. Nielsen (Eds.), *Optical Aspects of Oceanography* (pp. 1-24). New York: Academic
870 Press
871 Morel, A. (1980). In-water and remote measurements of ocean color. *Boundary-Layer*
872 *Meteorology,* 18/2, 177-201
873 Morel, A., & Antoine, D. (2007). Pigment Index Retrieval in Case 1 Waters. (25 p.),
874 Laboratoire d'Océanographie de Villefranche
875 Morel, A., Antoine, D., & Gentili, B. (2002). Bidirectional Reflectance of Oceanic
876 Waters: Accounting for Raman Emission and Varying Particle Scattering Phase
877 Function. *Appl. Opt.,* 41/30, 6289-6306
878 Morel, A., & Gentili, B. (1991). Diffuse reflectance of oceanic waters: Its dependence
879 on Sun angle as influenced by the molecular scattering contribution. *Appl. Opt.,* 30/30,
880 4427-4438
881 Morel, A., & Gentili, B. (1993). Diffuse reflectance of oceanic waters. II Bidirectional
882 aspects. *Appl. Opt.,* 32/33, 6864-6879
883 Morel, A., & Gentili, B. (1996). Diffuse reflectance of oceanic waters. III. Implication
884 of bidirectionality for the remote-sensing problem. *Appl. Opt.,* 35/24, 4850-4862
885 Morel, A., & Maritorena, S. (2001). Bio-optical properties of oceanic waters: A
886 reappraisal. *J. Geophys. Res.,* 106/C4, 7163-7180

887 Morel, A., & Prieur, L. (1977). Analysis of Variations in Ocean Color. *Limnology and*
888 *Oceanography,* 22/4, 709-722
889 Moses, W.J., Gitelson, A.A., Berdnikov, S., & Povazhnyy, V. (2009a). Estimation of
890 chlorophyll- a concentration in case II waters using MODIS and MERIS data -
891 successes and challenges. *Environmental Research Letters,* 4/4, 045005
892 Moses, W.J., Gitelson, A.A., Berdnikov, S., & Povazhnyy, V. (2009b). Satellite
893 Estimation of Chlorophyll-a Concentration Using the Red and NIR Bands of MERIS -
894 The Azov Sea Case Study. *Geoscience and Remote Sensing Letters, IEEE,* 6/4, 845-849
895 Murakami, H., Sasaoka, K., Hosoda, K., Fukushima, H., Toratani, M., Frouin, R.,
896 Mitchell, B., Kahru, M., Deschamps, P.-Y., Clark, D., Flora, S., Kishino, M., Saitoh, S.-
897 I., Asanuma, I., Tanaka, A., Sasaki, H., Yokouchi, K., Kiyomoto, Y., Saito, H., Dupouy,
898 C., Siripong, A., Matsumura, S., & Ishizaka, J. (2006). Validation of ADEOS-II GLI
899 ocean color products using in situ observations. *Journal of Oceanography,* 62/3, 373-
900 393
901 Nechad, B., Ruddick, K.G., & Park, Y. (2010). Calibration and validation of a generic
902 multisensor algorithm for mapping of total suspended matter in turbid waters. *Remote*
903 *Sensing of Environment,* 114/4, 854-866
904 Neukermans, G., Ruddick, K., Bernard, E., Ramon, D., Nechad, B., & Deschamps, P.-
905 Y. (2009). Mapping total suspended matter from geostationary satellites: a feasibility
906 study with SEVIRI in the Southern North Sea. *Opt. Express,* 17/16, 14029-14052
907 Nürnberg, G.K. (1996). Trophic State of Clear and Colored, Soft- and Hardwater Lakes
908 with Special Consideration of Nutrients, Anoxia, Phytoplankton and Fish. *Lake and*
909 *Reservoir Management,* 12/4, 432 - 447
910 O'Reilly, J.E., Maritorena, S., Mitchell, B.G., Siegel, D.A., Carder, K.L., Garver, S.A.,
911 Kahru, M., & McClain, C. (1998). Ocean color chlorophyll algorithms for SeaWiFS.
912 *Journal of Geophysical Research,* 103/C11, 24937-24953

913 Odermatt, D., Giardino, C., & Heege, T. (2010). Chlorophyll retrieval with MERIS
914 Case-2-Regional in perialpine lakes. *Remote Sensing of Environment,* 114/3, 607-617
915 Odermatt, D., Heege, T., Nieke, J., Kneubuehler, M., & Itten, K. (2008). Water quality
916 monitoring for Lake Constance with a physically based algorithm for MERIS data.
917 *Sensors,* 8/8, 4582-4599
918 Park, Y., & Ruddick, K. (2005). Model of remote-sensing reflectance including
919 bidirectional effects for case 1 and case 2 waters. *Appl. Opt.,* 44/7, 1236-1249
920 Petus, C., Chust, G., Gohin, F., Doxaran, D., Froidefond, J.-M., & Sagarminaga, Y.
921 (2010). Estimating turbidity and total suspended matter in the Adour River plume
922 (South Bay of Biscay) using MODIS 250-m imagery. *Continental Shelf Research,* 30/5,
923 379-392
924 Petzold, T.J. (1972). Volume scattering functions for selected ocean waters. *SIO Ref.*
925 *72–78* (79 p.), Scripps Institution of Oceanography, Univ. of Calif., San Diego
926 Pfeiffer, N., & Chapman, G.H. (2008). Successive order, multiple scattering of two-
927 term Henyey-Greenstein phase functions. *Opt. Express,* 16/18, 13637-13642
928 Piskozub, J., & McKee, D. (2011). Effective scattering phase functions for the multiple
929 scattering regime. *Opt. Express,* 19/5, 4786-4794
930 Pozdnyakov, D.V., Shuchman, R., Korosov, A., & Hatt, C. (2005). Operational
931 algorithm for the retrieval of water quality in the Great Lakes. *Remote Sensing of*
932 *Environment,* 97/3, 352
933 Preisendorfer, R.W. (1961). Application of Radiative Transfer Theory to Light
934 Measurements in the Sea. *International Union of Geodesy and Geophysics Monograph*
935 (pp. 11-29)
936 Qin, Y., Brando, V.E., Dekker, A.G., & Blondeau-Patissier, D. (2007). Validity of
937 SeaDAS water constituents retrieval algorithms in Australian tropical coastal waters.
938 *Geophys. Res. Lett.,* 34/21, L21603

939 Ruddick, K., Ovidio, F., & Rijkeboer, M. (2000). Atmospheric correction of SeaWiFS
940 imagery for turbid coastal and inland waters. *Applied Optics,* 39/6, 897-912
941 Ruddick, K.G., De Cauwer, V., Park, Y.-J., & Moore, G. (2006). Seaborne
942 measurements of near infrared water-leaving reflectance: The similarity spectrum for
943 turbid waters. *Limnology and Oceanography,* 51/2, 1167-1179
944 Santini, F., Alberotanza, L., Cavalli, R.M., & Pignatti, S. (2010). A two-step
945 optimization procedure for assessing water constituent concentrations by hyperspectral
946 remote sensing techniques: An application to the highly turbid Venice lagoon waters.
947 *Remote Sensing of Environment,* 114/4, 887-898
948 Sathyendranath, S., & Platt, T. (1997). Analytic model of ocean color. *Appl. Opt.,*
949 36/12, 2620-2629
950 Schalles, J.F., Gitelson, A.A., Yacobi, Y.Z., & Kroenke, A.E. (1998). Estimation of
951 chlorophyll-a from time series measurements of high spectral resolution reflectance in
952 an eutrophic lake. *Journal of Phycology,* 34/2, 383-390
953 Schroeder, T. (2005). *Fernerkundung von Wasserinhaltsstoffen in Küstengewässern mit*
954 *MERIS unter Anwendung expliziter und impliziter Atmosphärenkorrekturverfahren*.
955 Freie Universität Berlin: Doctoral thesis (in German)
956 Schroeder, T., Behnert, I., Schaale, M., Fischer, J., & Doerffer, R. (2007a). Atmospheric
957 correction algorithm for MERIS above case-2 waters. *International Journal of Remote*
958 *Sensing,* 28/7, 1469-1486
959 Schroeder, T., Schaale, M., & Fischer, J. (2007b). Retrieval of atmospheric and oceanic
960 properties from MERIS measurements: A new Case-2 water processor for BEAM.
961 *International Journal of Remote Sensing,* 28/24, 5627 - 5632
962 Schuchman, R.A., Korosov, A.A., Pozdnyakov, D.V., Means, J.C., Savage, S., Hatt, C.,
963 & Meadows, G.A. (2005). SeaWiFS and MODIS-observed multi-year seasonal and
964 spatial dynamics in biotic and abiotic processes in Lake Michigan as obtained from a

965 new water quality retrieval algorithm. *Proc. Proc. of 31st Int. Symp. on Remote Sensing*
966 *of Environment*, St. Petersburg, Russia
967 Shanmugam, P., Ahn, Y.-H., Ryu, J.-H., & Sundarabalan, B. (2010). An evaluation of
968 inversion models for retrieval of inherent optical properties from ocean color in coastal
969 and open sea waters around Korea. *Journal of Oceanography,* 66/6, 815-830
970 Shuchman, R., Korosov, A., Hatt, C., Pozdnyakov, D., Means, J., & Meadows, G.
971 (2006). Verification and Application of a Bio-optical Algorithm for Lake Michigan
972 Using SeaWiFS: a 7-year Inter-annual Analysis. *Journal of Great Lakes Research,* 32/2,
973 258-279
974 Siegel, D.A., Wang, M., Maritorena, S., & Robinson, W. (2000). Atmospheric
975 correction of satellite ocean color imagery: The black pixel assumption. *Applied Optics,*
976 39/21, 3582-3591
977 Smith, R.C., & Baker, K.S. (1981). Optical properties of the clearest natural waters
978 (200-800 nm). *Applied Optics,* 20/, 177-
979 Sokolov, A., Chami, M., Dmitriev, E., & Khomenko, G. (2010). Parameterization of
980 volume scattering function of coastal waters based on the statistical approach. *Opt.*
981 *Express,* 18/5, 4615-4636
982 Stumpf, R.P., Arnone, R.A., Gould, R.W., Martinolich, P.M., & Ransibrahmanakul, V.
983 (2003). A partially coupled ocean-atmosphere model for retrieval of water-leaving
984 radiance from SeaWiFS in coastal waters. In: *SeaWiFS Postlaunch Tech. Rep. Ser.*, *22*
985 (51-59 p.), S.B. Hooker & E.R. Firestone (Eds.), NASA Goddard Space Flight Cent.
986 Sullivan, J.M., & Twardowski, M.S. (2009). Angular shape of the oceanic particulate
987 volume scattering function in the backward direction. *Appl. Opt.,* 48/35, 6811-6819
988 Sydor, M. (2007). Statistical Treatment of Remote Sensing Reflectance from Coastal
989 Ocean Water: Proportionality of Reflectance from Multiple Scattering to Source
990 Function b/a. *Journal of Coastal Research*, 1183-1192

991 Toratani, M., Fukushima, H., Murakami, H., & Tanaka, A. (2007). Atmospheric
992 correction scheme for GLI with absorptive aerosol correction. *Journal of*
993 *Oceanography,* 63/3, 525-532
994 Tyler, A.N., Svab, E., Preston, T., Présing, M., & Kovács, A. (2006). Remote sensing of
995 the water quality of shallow lakes: A mixture modelling approach to quantifying
996 phytoplankton in water characterized by high-suspended sediment. *International*
997 *Journal of Remote Sensing,* 27/8, 1521
998 Van der Woerd, H., & Pasterkamp, R. (2004). Mapping of the North Sea turbid coastal
999 waters using SeaWiFS data. *Canadian Journal of Remote Sensing,* 30/1, 44-53
1000 Van Der Woerd, H.J., & Pasterkamp, R. (2008). HYDROPT: A fast and flexible
1001 method to retrieve chlorophyll-a from multispectral satellite observations of optically
1002 complex coastal waters. *Remote Sensing of Environment,* 112/4, 1795-1807
1003 Vasilkov, A., & Kopelevich, O. (1982). The reasons of maximum at about 700 nm on
1004 radiance spectra of the sea. *Oceanology,* 22/, 945-950
1005 Vidot, J., & Santer, R. (2005). Atmospheric correction for inland waters - application to
1006 SeaWiFS. *International Journal of Remote Sensing,* 26/17, 3663
1007 Vos, W.L., Donze, M., & Buiteveld, H. (1986). On the reflectance spectrum of algae in
1008 water: The nature of the peak at 700 nm and its shift with varying concentration. In:
1009 *Communication on Sanitary Engineering and Water Management* (86-122 p.)
1010 Wang, J.-J., Lu, X.X., Liew, S.C., & Zhou, Y. (2009). Retrieval of suspended sediment
1011 concentrations in large turbid rivers using Landsat ETM+: an example from the Yangtze
1012 River, China. *Earth Surface Processes and Landforms,* 34/8, 1082-1092
1013 Wang, J.J., & Lu, X.X. (2010). Estimation of suspended sediment concentrations using
1014 Terra MODIS: An example from the Lower Yangtze River, China. *Science of The Total*
1015 *Environment,* 408/5, 1131-1138

1016 Wang, M. (2007). Remote sensing of the ocean contributions from ultraviolet to near-
1017 infrared using the shortwave infrared bands: simulations. *Appl. Opt.,* 46/9, 1535-1547
1018 Wang, M., Shi, W., & Tang, J. (2011). Water property monitoring and assessment for
1019 China's inland Lake Taihu from MODIS-Aqua measurements. *Remote Sensing of*
1020 *Environment,* 115/3, 841-854
1021 Werdell, P.J., Bailey, S.W., Franz, B.A., Harding Jr, L.W., Feldman, G.C., & McClain,
1022 C.R. (2009). Regional and seasonal variability of chlorophyll-a in Chesapeake Bay as
1023 observed by SeaWiFS and MODIS-Aqua. *Remote Sensing of Environment,* 113/6,
1024 1319-1330
1025 Wetzel, R.G. (1983). *Limnology*. Philadelphia: W.B. Saunders Co.
1026 Witter, D.L., Ortiz, J.D., Palm, S., Heath, R.T., & Budd, J.W. (2009). Assessing the
1027 Application of SeaWiFS Ocean Color Algorithms to Lake Erie. *Journal of Great Lakes*
1028 *Research,* 35/3, 361-370
1029 Yang, W., Matsushita, B., Chen, J., & Fukushima, T. (2011). Estimating constituent
1030 concentrations in case II waters from MERIS satellite data by semi-analytical model
1031 optimizing and look-up tables. *Remote Sensing of Environment,* 115/5, 1247-1259
1032 Zhai, P.-W., Hu, Y., Chowdhary, J., Trepte, C.R., Lucker, P.L., & Josset, D.B. (2010).
1033 A vector radiative transfer model for coupled atmosphere and ocean systems with a
1034 rough interface. *Journal of Quantitative Spectroscopy and Radiative Transfer,* 111/7-8,
1035 1025-1040
1036 Zhang, M., Tang, J., Dong, Q., Song, Q., & Ding, J. (2010). Retrieval of total suspended
1037 matter concentration in the Yellow and East China Seas from MODIS imagery. *Remote*
1038 *Sensing of Environment,* 114/2, 392-403
1039 Zhou, W., Wang, S., Zhou, Y., & Troy, A. (2006). Mapping the concentrations of total
1040 suspended matter in Lake Taihu, China, using Landsat-5 TM data. *International*
1041 *Journal of Remote Sensing,* 27/6, 1177-1191